Fatigue Analysis of RC Slabs Reinforced with Plain Bars Based on the Bridging Stress Degradation Concept

Ahmed Attia Drar, Takashi Matsumoto

Journal of Advanced Concrete Technology, volume 14 (2016), pp. 21-34

Scientific paper

Fatigue Analysis of RC Slabs Reinforced with Plain Bars Based on the Bridging Stress Degradation Concept

Ahmed Attia M. Drar[1*] and Takashi Matsumoto[2*]

Received 24 September 2015, accepted 5 January 2016 doi:10.3151/jact.14.21

Abstract

There is an increasing demand from researchers and engineers to know the fatigue behaviors of RC bridge slabs under a moving load. Therefore, many numerical and experimental studies have been conducted to predict the fatigue life of these slabs. Most of these studies focused on the modeling of fatigue behaviors of RC slabs reinforced with deformed bars. However, many RC slabs in use today are reinforced with plain bars, and they are suffering from fatigue damages. A numerical method based on the bridging stress degradation concept is presented in this study to simulate the fatigue behaviors of RC slabs reinforced with plain bars under a moving load. The bond-slip effect between a reinforcing bar and its surrounding concrete is taken into consideration by adding equivalent bond strain to plain bar strain. The numerical model is verified using previous experimental data. This model is also able to capture the cracking pattern, change in displacement and rebar strain. The numerical results provide a good agreement with the experimental ones.

1. Introduction

Researchers and structural designers are concerned about the safety of construction in the long-term. Reinforced concrete (RC) bridge-deck slabs are subjected to a repetition of moving loads. These structures are required to avoid the fatigue failure. Therefore, there is a growing necessity to know fatigue life and performance of RC slabs. Accurate modeling of the fatigue behaviors of RC slabs is considered to be essential for the prediction of fatigue life.

Many research groups have conducted experiments to investigate the fatigue behaviors of RC slabs. Previous studies (Matsui 1978; Perdikaris and Beim 1988) found that the fatigue life of RC slabs under a moving load is lower than that under a fixed pulsating load. In these experimental studies, the most common mode of fatigue failure was by punching shear mode. Recently, numerical studies have been presented regarding RC structures subjected to repetitive loading to predict fatigue behaviors. Ueda *et al*. (1999) analyzed the fatigue strength of steel-concrete sandwich beams using the finite element method (FEM). Tailored constitutive models were employed according to fatigue effects by reducing stiffness and strength of material models. This reduction is mainly based on the empirical formulations from previous experimental analyses. This investigation indicated that the effect of reduction in compressive stiffness was found to be negligible. Maekawa *et al*. (2006) presented a numerical fatigue simulation of RC slabs under a moving load. This numerical method used a direct path-integral scheme with fatigue constitutive models for concrete tension, compression and crack surfaces shear. The fatigue deterioration of RC slabs under moving load is significant when the concrete fatigue modeling based on a reduction of shear transfer and tension stiffness is considered.

The above-mentioned works concluded that the tension fatigue modeling for concrete plays an important role in predicting the fatigue behaviors of RC slabs. Therefore, understanding a mechanism of fatigue crack propagation is essential to evaluate concrete fatigue representation in tension. The bridging stress degradation concept was introduced for the first time by Li and Matsumoto (2006) as a principal cause of fatigue crack propagation in concrete and fiber reinforced concrete beams. Suthiwarapirak and Matsumoto (2006) used this concept in their numerical model to predict the fatigue behaviors of RC slabs. This study successfully provided a fatigue analysis of RC slabs under moving and fixed pulsating loads.

Until 1965, the plain bars are used for reinforcing RC bridge slabs. These slabs have been serviced more than 50 years. An example of RC slab reinforced with plain bars is seen in Xuan-bridge (national highway No. 334, Shari, Hokkaido, Japan) which was built in 1964. This bridge is suffering from fatigue damage due to a huge number of moving load repetitions. The fatigue damage significantly existed in the RC slab reinforced with plain bars than that reinforced with deformed bars. Therefore, it is essential to find a method for prediction of fatigue life and choosing a repairing strategy for RC slabs reinforced with plain bars.

For RC slabs reinforced with plain bars, an experi-

[1]Doctoral student, Graduate School of Engineering, Division of Engineering and Policy for Sustainable Environment, Hokkaido University, Sapporo, Japan.
*Corresponding author, *E-mail:* attya85@yahoo.com
[2]Professor, Faculty of Engineering, Division of Engineering and Policy for Sustainable Environment, Hokkaido University, Sapporo, Japan. *Corresponding author, *E-mail:* takashim@eng.hokudai.ac.jp

Table 1 Constitutive laws for concrete (Maekawa *et al*. 2003).

Compression		Tension*	
$0 \geq \varepsilon \geq \varepsilon_m$	$\sigma = f_c \frac{\varepsilon}{\varepsilon_m}\left(2 - \frac{\varepsilon}{\varepsilon_m}\right)$	$\varepsilon_t \geq \varepsilon \geq 0$	$\sigma = E_c \varepsilon$
$\varepsilon_m \geq \varepsilon \geq \varepsilon_u$	$\sigma = f_c \frac{\varepsilon_u - \varepsilon}{\varepsilon_u - \varepsilon_m}$	$\varepsilon > \varepsilon_t$	$\sigma = f_t \left(\frac{\varepsilon_t}{\varepsilon}\right)^{0.4}$

E_c = the modulus of elasticity of concrete, f_c = concrete compressive strength, $\varepsilon_m = f_c/2E_c$ = concrete strain corresponding f_c, f_t = tensile strength, and $\varepsilon_t = f_t/E_c$ = strain at tensile strength.
*The multiplier 0.4 can be used for the concrete reinforced with deformed bars.

mental study on the fatigue durability was conducted by Shakushiro *et al*. (2011) to propose an empirical formula for the fatigue life evaluation of these slabs. Although many existing RC slabs in use are reinforced with plain bars, analytical study for the fatigue life of these slabs has been rarely conducted. Therefore, it is necessary to accurately simulate fatigue behaviors numerically and develop the method of fatigue life prediction for the RC slabs reinforced with plain bars.

This study presents a numerical method to simulate the fatigue behaviors of the RC slabs reinforced with plain bars under a moving load. The experimental study by Shakushiro *et al*. (2011) is used to verify the analytical results in static (Shakushiro 2014) and fatigue loading. The bridging stress degradation concept is employed in this numerical method to simulate the deterioration of concrete under repetitive load. The bond-slip effect between a plain reinforcing bar and its surrounding concrete is carefully taken into consideration. Furthermore, fatigue life, slab center displacement evolution and rebar strain are shown in this study. The comparison of fatigue behaviors between RC slab reinforced with plain bars and that reinforced with deformed bars is also provided.

2. Method

2.1 Concrete

For concrete, an FEM based on the Newton-Raphson iteration scheme is employed for getting a solution of the effective stiffness matrix. Nonlinear constitutive laws of concrete are shown in **Table 1**. The bridging stress relation, which is the transferred stress between crack surfaces through aggregates, is introduced to represent the cracking behavior of concrete. Crack propagation characteristics of concrete are adapted by 8-node 3D smeared crack elements with multiple fixed crack concepts (Rots and Blaauwendraad 1989). For cracked elements, the first crack is assumed to start perpendicular to the direction of the maximum principal strain in the concrete matrix when tensile strain is larger than the cracking strain as shown in **Fig. 1(a)**. After the first crack appears, the second crack can propagate perpendicular to the first crack when the second tensile strain component exceeds the cracking strain. In addition, the third crack can form perpendicularly to the existing two cracks as shown in **Fig. 1(b)**.

The bridging stress degradation characteristic of concrete under a repetitive load is the most important part in the current fatigue analysis. A crack starts with length, a, and width, w, due to the first loading as shown in **Fig. 2(a)**. Repetitive loading leads to the reduction of bridging stress, because the crack is subjected to a process of opening and closing. Therefore, this crack propagates with additional length, da, and additional width, dw, as shown in **Fig. 2(b)**. This reduction is defined as the bridging stress degradation concept, and it is assumed to depend on two parameters: maximum tensile strain, $\varepsilon_{t\max}$, and number of cycles, N (Li and Matsumoto 1998). The equation of bridging stress degradation can be expressed as (Jun and Stang 1998):

$$\frac{\sigma_N}{\sigma_1} = 1 - (d_0 + k\varepsilon_{t\max} l)\log(N) \quad (1)$$

where l is cracked element size, d_0 is stress degradation factor, k is slope of the linear relation between the bridg-

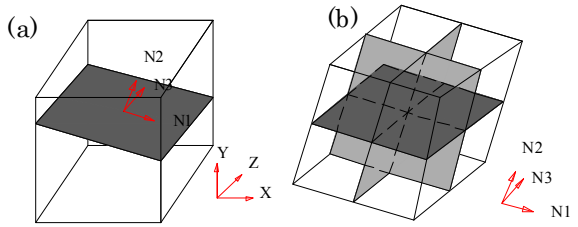

Fig.1 Crack formation: (a) initiation of a first crack; (b) three perpendicular crack formations.

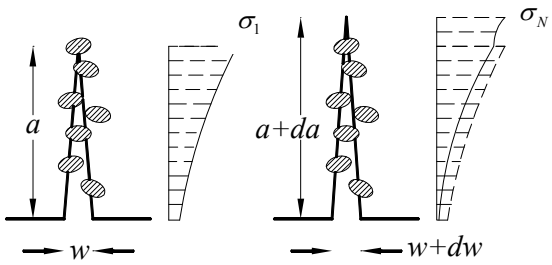

Fig.2 Crack propagation due to bridging stress: (a) the first cycle; (b) after N cycles.

ing degradation factor and maximum tensile strain, $\varepsilon_{t\max}$, σ_N and σ_1 are bridging stress at the *N*th and the first cycle, respectively. Zhang *et al*. (1999, 2000) analyzed a large number of experimental data to conclude that the degradation of crack bridging stress under cyclic load is controlled by the number of cycle and the maximum and minimum crack opening. This degradation can be fitted by a linear model as a function of the logarithm of the number of cycles as shown in equation (1). As Zhang *et al*. (1999, 2000), this factor can be approximately related to the maximum crack opening. Through their studies, it is found that $d_0 = 0.08$ and $k = 4$ mm^{-1} when the crack opening ≤ 0.016 mm and $d_0 = 0.014$ and $k = 0.12$ mm^{-1} when the crack opening > 0.016 mm. For smeared crack elements, the bridging stress degradation occurs by multiple cracks. Therefore, first range (the crack opening ≤ 0.016 mm) is applicable in this study (Suthiwarapirak and Matsumoto 2006).

The bridging stress in concrete is mainly influenced by the maximum particle size and surface texture of aggregate. The effect of aggregate size on bridging stress was studied by Wolinksi *et al*. (1987). This study found that the maximum bridging stress and fracture energy are almost the same for concrete comprising mixes with maximum aggregate particle size of 8 mm, 16 mm and 32 mm. Therefore, this equation can be used to verify the experimental results by Shakushiro *et al*. (2011) which used aggregate of maximum aggregate particle size of 20 mm.

2.2 Reinforcement bar

The reinforcement of RC slabs is modeled as a smeared rebar with its reinforcement ratio distributed in any desired direction. The stress-strain relationship of reinforcement is represented by a bilinear curve with explicit yield stress, f_y. For RC elements reinforced with plain bars, the bond effect between a plain reinforcing bar and its surrounding concrete is considered as the most influential factor to obtain a reliable simulation (Varum 2003). Therefore, it is important to consider the bond-slip effect during analysis. The modified steel bar model by Dehestani and Mousavi (2015) is employed in this method to simulate the bond-slip effect on the stress-strain ($\sigma - \varepsilon$) relationship under a monotonic loading. This modification contains the addition of equivalent bond strain to reinforcing bar strain as shown in **Fig. 3**. This leads to a decrease in the effective stiffness of the rebar model and an increase in its deformations. To describe the assumption of this method, an RC element in bending is considered as shown in **Fig. 4**. There is no tensile stress in concrete at cracked section and the reinforcing bar transfers the tension force. However, the concrete between cracks participates in the tensile strength of the overall RC cross section. The concrete located between cracks can be divided to three main parts as shown in **Fig. 4**. In cracked section, there is no bond stress between the reinforcement and its surrounding concrete. The transmission length of bond stress, l_d, is located between the cracked section and the perfect bond zone. This method can be tailored for plain bars to obtain the effective stiffness, E_s^*, as follows.

$$E_s^* = \frac{f_y^*}{\varepsilon_y^*}, \tag{2}$$

$$\varepsilon_y^* = \varepsilon_y + \frac{S_y}{l_d}, \tag{3}$$

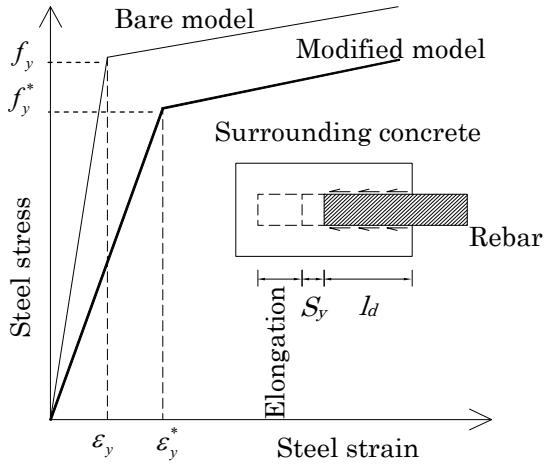

Fig.3 Reinforcing bar model.

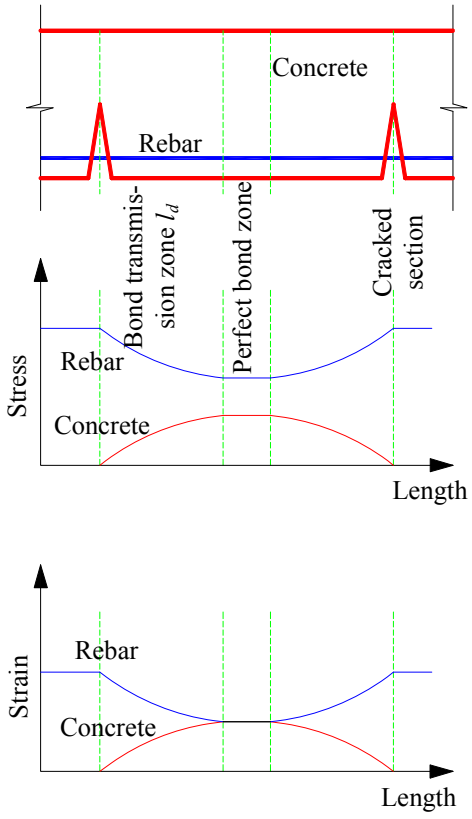

Fig.4 Stress and strain distribution of a cracked RC element in bending.

Table 2 RC slabs details.

Slab ID	Loading type (kN)	Concrete properties (MPa)		Yield strength of Reinforcement (MPa)
		Strength	Stiffness	
S	Static	39.9	24300	235 (Plain)
P110	Moving (110)	43	25900	
P150	Moving (150)	41.7	25400	
P190	Moving (190)	36.6	26000	
D150	Moving (150)	38.6	23900	345 (Deformed)

$$S_y = 0.4\left(\frac{d_b}{4}\cdot\frac{f_y}{\sqrt{f_c'}}\cdot(2\alpha+1)\right)^{1/\alpha} + 0.34, \quad (4)$$

$$l_d = \frac{d_b \cdot f_y}{4\cdot\tau_b} \quad (5)$$

where f_y^* is the effective yield stress (Belarbi and Hsu 1994), S_y is the slip displacement of a steel bar at yield point (Zhao and Sritharan 2007), d_b is the rebar diameter, f_c' is the concrete compressive strength, α is a tuning parameter used for adjusting the local bond stress-slip relationship = 0.5 for plain bar (Melo *et al*. 2011), τ_b is the average bond stress, ε_y and ε_y^* are the explicit and effective yield strain, respectively.

The effective stiffness degradation of plain bar due to a repetitive load is not taken into consideration in this study. Therefore, the reduction of rebar stiffness due to an applied load is the major effect on the RC element behaviors at first cycle. While, the bridging stress degradation in concrete plays the most important role in other cycles.

For RC elements reinforced with deformed bars, the bond between a non-yielded deformed bar and its surrounding concrete is assumed to be perfect. In other words, the slip displacement of a deformed bar at yielding is considered as zero ($S_y \approx 0$). Moreover, its bond degradation due to a repetitive load is not considered in this study. Since there is no report of RC slab failure due to fatigue rupture of reinforcing bar, this study focused on the concrete deterioration due to repetitive loading. For plain bar, the stiffness reduction at first cycle results in an increasing of concrete strain. According to equation (1), this leads to a significant concrete degradation than that in deformed bar.

The Giuffré-Menegotto-Pinto model (Menegotto and Pinto 1973) is employed to represent the hysteretic behavior of a rebar under repetitive load as following:

$$\frac{\sigma}{f_y^*} = H\frac{\varepsilon}{\varepsilon_y^*} + \frac{(1-H)\dfrac{\varepsilon}{\varepsilon_y^*}}{\left[1+\left(\dfrac{\varepsilon}{\varepsilon_y^*}\right)^R\right]^{1/R}}, \quad (6)$$

$$R = R_0 - \frac{a_1\xi_{\max}}{a_2 - \xi_{\max}}, \quad (7)$$

where H is the strain hardening parameter, R_0, and R are the transition parameter between elastic and hardening for the first and Nth cycle (R_0 =20), $\xi_{\max}$ is the maximum excursion in plastic range, a_1 and a_2 are the parameters for the change of R with repetitive load history, equal to 18.5 and 0.00015, respectively.

2.3 RC slab modeling and analytical procedures

To verify the method explained in the preceding sections, an RC slab model of smeared crack elements is solved. The loading pattern and load levels are the same as those used in the experiments (Shakushiro *et al*. 2011). All slabs were supported by steel I-beams and hinged supports along its longitudinal and transverse directions, respectively. The concrete and reinforcement properties of these slabs are the same as those used in the experimental study. The details of these tested slabs are shown in **Table 2** (Shakushiro *et al*. 2011). For static analysis, a distributed load with a size of 120 × 300 mm is applied at 780 mm from the slab center to check the punching shear behavior as shown in **Fig. 5(a)**. For fatigue analysis, a moving load was simulated by moving a constant load level along the longitudinal direction as shown in **Fig. 5(b)**.

The fatigue analysis was conducted as shown in **Fig. 6(a)**. Firstly, a moving load is applied at the center of the slab elements. Then, these elements are unloaded, while other elements, adjacent to the right side of the loaded elements, are loaded simultaneously with equal increments. In this technique, a constant load is made to move along longitudinal directions. Due to the symmetry, only half of the model is analyzed. This loading leads to the propagation of cracked elements in the first cycle as shown in **Fig. 6(b)**. By increasing the number of cycles, the constitutive laws of cracked elements are modified according to the bridging stress degradation concept. This leads to the loss of tensile stress in these cracked elements resulting a stress concentration at crack tip. Therefore, new cracked elements are propagated around this stress concentration as shown in **Fig. 6(c)**. According to this propagation and the bridging stress degradation of these cracked elements, the overall RC slab stiffness decreases with an increasing number of cycles. At different moving load locations, the output-cracked elements were stored to be used in updating the numerical model for the next cycle step. This procedure is repeated in each cycle until fatigue failure occurs, while the numerical results are recorded in each cycle.

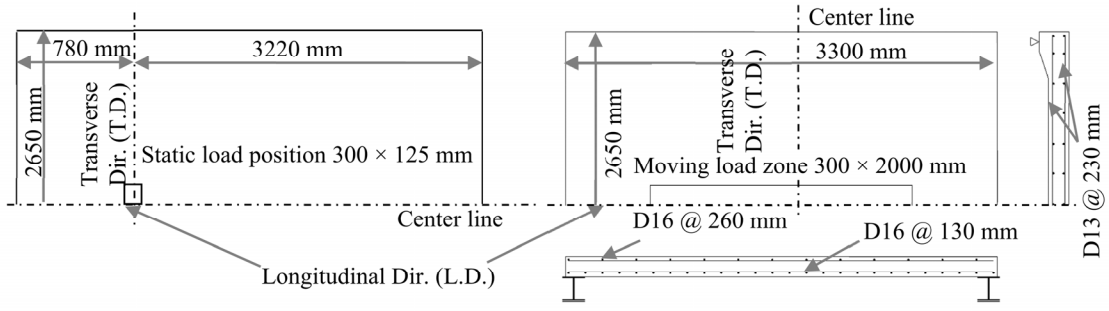

(a) RC slab under static load (b) RC slab under moving load

Fig.5 RC slab geometry.

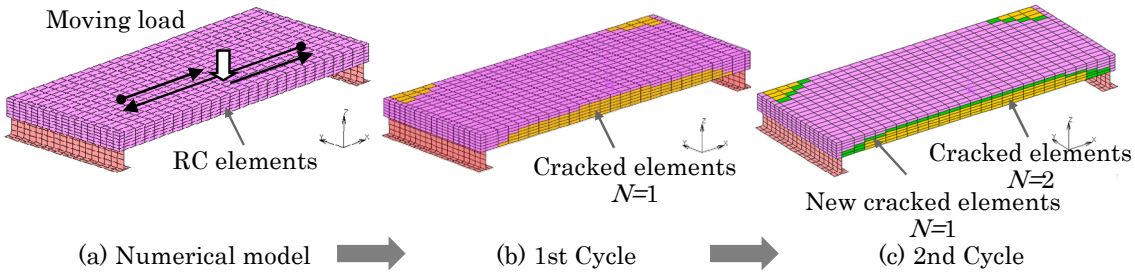

Fig.6 Analytical procedures.

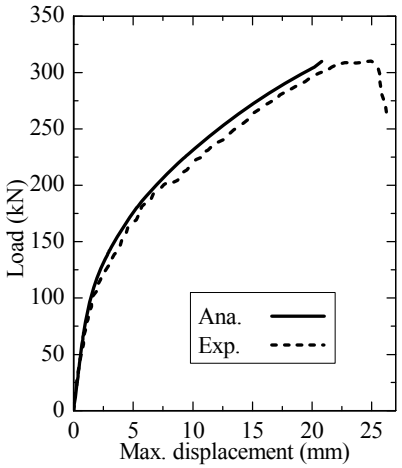

Fig.7 Load-maximum displacement curves.

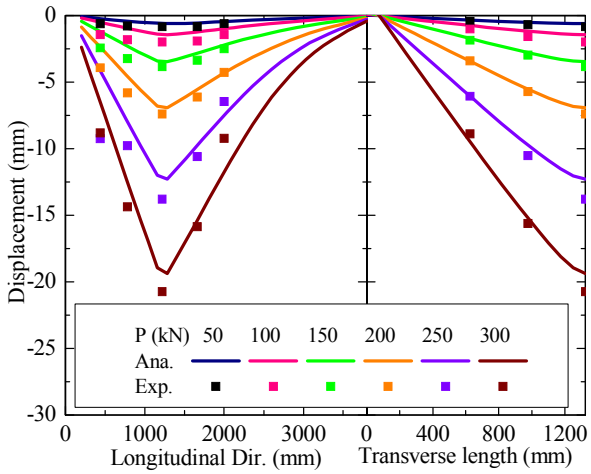

Fig.8 Displacement distribution for longitudinal and transverse direction.

According to this technique, a repetition of moving load leads to the loss of sectional moment balance. The fatigue failure occurs when the equilibrium cannot be exceeded with the deteriorated cracked elements. Hence, the cracked elements are propagated rapidly resulting a significant decreasing of slab stiffness. This leads to an accelerated increasing of slab displacement indicating to a fatigue failure.

3. Results and discussion

To verify this numerical method, static and fatigue analyses were conducted on five full-scale RC slabs to compare them with the experimental results in Shakushiro *et al*. (2011) as follows.

3.1 Displacement due to static loading

Displacement was measured at the loading point. The load-maximum displacement relationship of an RC slab under static load is shown in **Fig. 7**, and it exhibits a good agreement with the experimental one. At a load more than 75 kN, RC slab stiffness decreased gradually due to the propagation of cracks. Finally, the static ultimate load of this slab became equal to 309 kN.

At different load levels, the displacements of various points were experimentally measured by Shakushiro (2014). The comparison of displacement distributions along the longitudinal and transverse directions between the experiment and the numerical model at different applied load levels is shown in **Fig. 8**. This comparison

represents an acceptable agreement between them. As shown in this figure, the maximum displacement of the numerical model is located under the loading point.

The distribution of maximum principal tensile strain on the bottom of the RC slab at failure is shown in **Fig. 9**. This figure presents only half of the slab due to symmetry in longitudinal direction. This figure shows the strain concentration under the loading point indicating that the cracks are localized at this point. This observation can be considered as an indication of punching shear failure. This agrees with the experimental results of the RC slabs under static loading (Shakushiro 2014).

3.2 Propagation of cracked elements

This numerical method considers the fundamental factor that the propagation and degradation of cracked elements are the main causes of fatigue failure. Therefore, it is important to describe the propagation of cracked elements. The propagation of cracked elements of the RC slabs under a moving load at different numbers of cycles is shown in **Fig. 10**. The one fourth of a slab model is shown due to the symmetry in both directions. As shown in this figure, uncolored elements point to a non-cracked zone. The cracked zone caused by the first cycle of the moving load is indicated in blue, while the cracked zones caused by further cycles are indicated by other colored elements. In all slabs, the transverse direction (T.D.) shows the propagation of cracked elements that extend from the center of the loading area, whereas the longitudinal direction (L.D.) shows the cracked elements that distribute all over the movement zone. In other words, the cracked zone in the longitudinal direction is larger than that in the transverse direction. The reason is that the movement effect of load was transmitted along the longitudinal direction.

To explicate the propagation effect of these cracked elements on fatigue life, the size of the cracked zone after the first cycle (blue color elements) is considered as an indication of the fatigue life of these slabs. For example, the cracked zone at the first cycle of P110 is smaller than that of other slabs. Therefore, this slab needs more cycles to propagate additional cracked zones until fatigue failure occurs compared with the

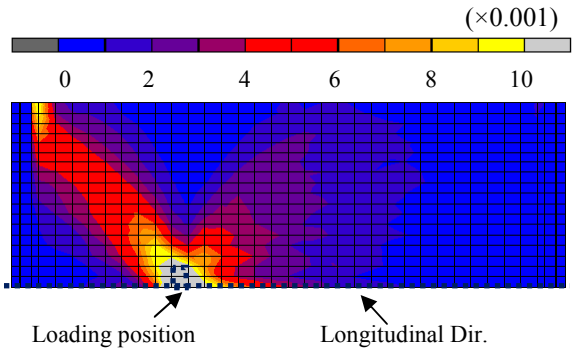

Fig.9 Maximum principal tensile strain on bottom surface of RC slab under static loading at failure (load = 309 kN).

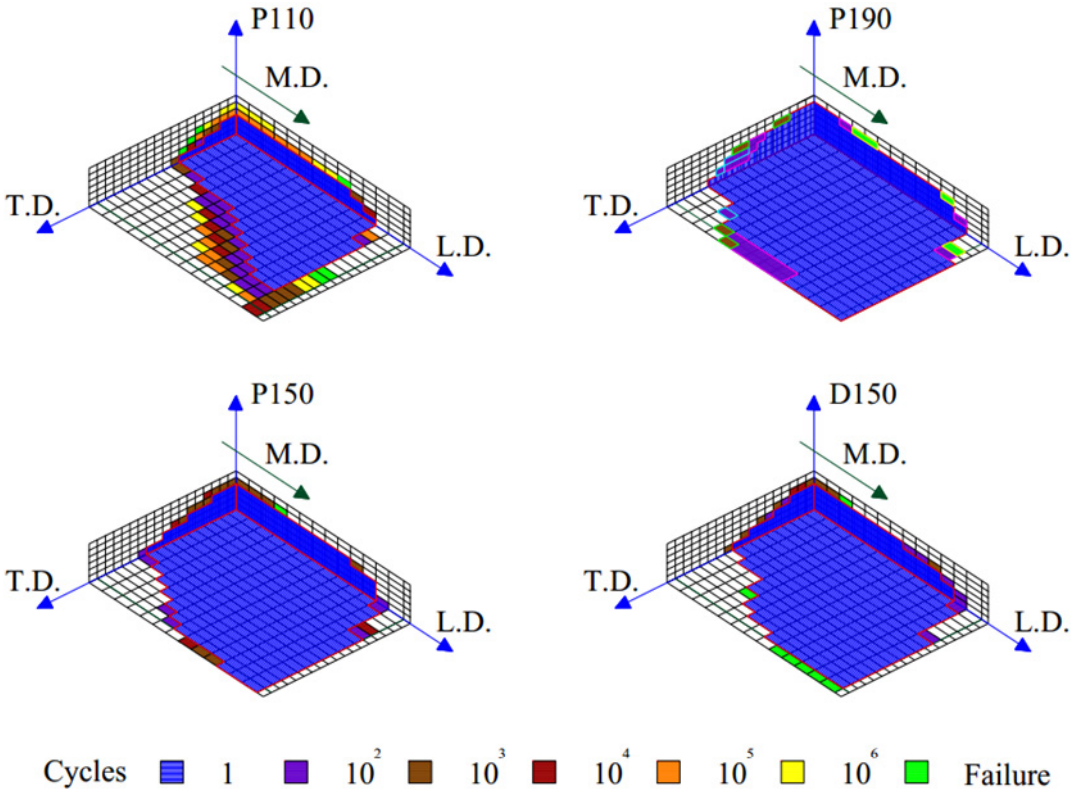

M.D.: Moving Dir. L.D.: Longitudinal Dir. T.D.: Transverse Dir.

Fig.10 Propagation of cracked elements.

other slabs. Moreover, cracked elements at the first cycle were subjected to crack closing and opening processes more than those at the additional cycles. According to equation (1), these cracked elements deteriorated more than the cracked elements at later cycles with an increasing number of cycles. Therefore, P190, which shows the largest cracked zone at the first cycle, deteriorated more quickly than the other slabs.

According to the percentages of cracked elements volume in **Table 3**, the propagation of the cracked elements observed in D150 and P150 show that D150, which was reinforced with deformed bars, resulted in a slightly smaller cracked zone at the first cycle than P150, which was reinforced with plain bars. However, this observation is significant at the fatigue failure indicating a higher average degradation ratio for P150 than that of D150. The average degradation ratio is the ratio of the difference between the cracked elements volume at fatigue failure and 1st cycle by mm^3 to the fatigue life by cycles. The reason is that the bond effect between a plain bar and its surrounding concrete leads to larger slab deformations than that between a deformed bar and its surrounding concrete. This leads to a higher maximum tensile strain, $\varepsilon_{t\max}$, for P150 than that of D150. According to equation (1), the concrete bridging stress of P150 deteriorated more than that of D150 causing a larger cracked zone and a smaller fatigue life for P150. Shakushiro *et al*. (2011) used the damaged area of the bottom slab surface to evaluate the fatigue failure. However, the cracked elements propagation in the thickness direction is consider as a primary factor for fatigue failure. Therefore, this study consider the percentage of cracked elements volume as a suitable comparison tool for these slabs.

For all slabs, the cracked elements are vertically propagated with an increasing number of cycles. At fatigue failure, the non-cracked zones are located at the top of the slab, until one-sixth of slab thickness. Therefore, a repetition of moving load leads to a decreasing of a compression zone. This approaches to an unequal sectional stress distribution resulting a fatigue failure.

Table 3 The percentage of the cracked elements volume.

Slab ID	The cracked elements volume%		Average degradation ratio (mm^3/Cycle)
	1st cycle	Failure	
P110	12%	40.8%	91
P150	33.4%	59.1%	7070
P190	57.2%	68.6%	23456
D150	32.6%	51%	2575

3.3 Center displacement evolution

The propagation of cracked elements and its degradation indicate that the RC slab stiffness decreases and slab center displacement increases as the number of cycles increases. The center displacement evolution versus the number of cycles for all slabs is compared with the experimental results in **Fig. 11**. The slab under a higher moving load level shows a larger slab center displacement than that under a lower moving load level due to the initial displacement at first cycle. In addition, at a higher moving load level, the center displacement evolution shows a larger slope than that at a lower moving load level. The reason is that the slab under a higher moving load level deteriorated more quickly than that at lower moving load level. According to reinforcing bars modeling, the center displacement evolution of RC slab reinforced with deformed bars, D150, is smaller than that reinforced with plain bars, P150.

This figure shows the comparison of center displacement evolutions between the experimental and analytical results at different moving load levels. It reveals similar values for fatigue life and center displacement, indicating an acceptable agreement between them.

3.4 Fatigue life and S-N relationship

The fatigue life of RC slabs is described as a relationship between fatigue load ratio and the number of cycles to failure. The ratio of an applied moving load to the ultimate static load is considered as the fatigue load ratio, *S*. The S-N relationship of RC slabs under a moving load is plotted with the experimental results for veri-

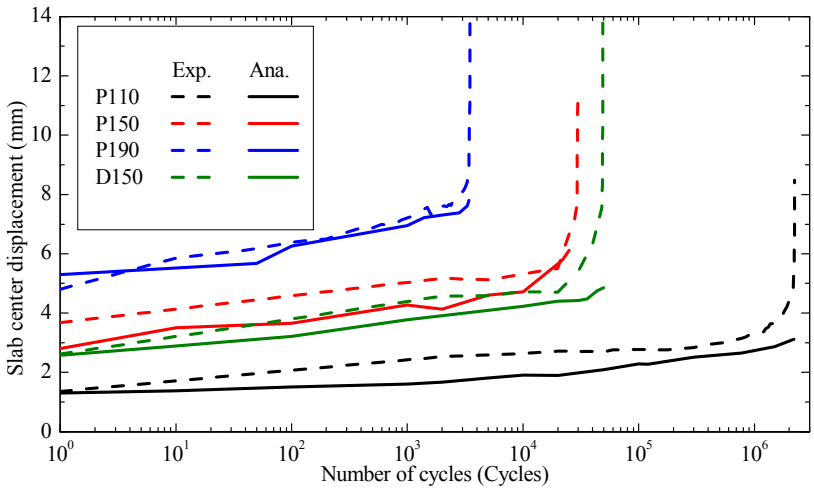

Fig.11 Center displacement evolutions.

fication as shown in **Fig. 12**. It suggests a good agreement between the analytical results of RC slabs and the fatigue life of those slabs from the experiment. Due to the propagation of cracked elements, the RC slab subjected to a higher fatigue load ratio shows a shorter fatigue life than that at a lower fatigue load ratio. The fatigue life of theses slabs is listed in **Table 4**.

3.5 Cracking patterns due to a moving load and fatigue failure

To examine the crack locations in the numerical model, the cracking pattern on bottom surface of RC slabs under a moving load at fatigue failure is compared with the experimental results as shown in **Fig. 13**. For all slabs, the main crack started at its center, the first location of the moving load, thereafter extending to the supporting corners. As the load began to move, diagonal cracks formed between the locations of the moving load in the longitudinal direction and the supporting corner, making the first crack set. At the same time, other cracks formed perpendicular to the existing cracks as the second and third crack sets, surrounding the moving load zone to create an ellipse shape. An increase in the number of cycles resulted in much more extensive cracking.

As shown in **Fig. 13**, the effect of increasing the moving load level on the cracking pattern appears to be wide-ranging. The cracking pattern at fatigue failure contains an initial damage at the first cycle and accumulated damage by moving loading. The initial damage at the first cycle is influenced by moving load value. Moreover, applying higher moving load level leads to an increasing of maximum tensile strain, $\varepsilon_{t\max}$, in equation (1). By increasing number of cycles, this leads to a significant bridging stress degradation and an increasing in degradation ratio as shown in **Table 3** resulting a wide-ranging in cracking pattern. An observation of the cracking patterns for P150 and D150 shows that the RC slab reinforced with plain bars suffered more broad-distribution cracking than that reinforced with deformed bars. The reason is that the bond effect between a plain bar and its surrounding concrete leads to a greater principal strain than that reinforced with deformed bars. However, the experimental cracking pattern for the RC slab reinforced with deformed bars shows an extensive cracking than that reinforced with plain bars. The reason is that the crack spacing of the RC slab reinforced with deformed bars is smaller than that reinforced with plain bars due to its shorter bond-deterioration length. On the other hand, the numerical crack spacing is controlled by the element size. Therefore, this observation cannot be detected in the numerical results. All cracking patterns and cracked elements distribution in the transverse direction suggest that these slabs failed with the punching shear mode around the moving area. This failure mode can be observed in the experiments. According to this observation, numerical cracking patterns show a good agreement with the experiments.

Table 4 Fatigue life of RC slabs.

Slab ID	Fatigue life (Cycles)	
	Numerical	Experimental (Shakushiro *et al*. 2011)
P110	2,200,000	2,220,000
P150	25,500	29,800
P190	3,400	3,506
D150	50,000	48,916

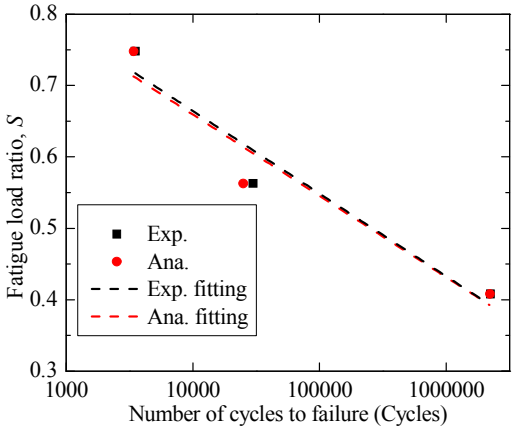

Fig.12 S-N relationships for RC slabs reinforced with plain bars.

To demonstrate the fatigue failure mechanism, the maximum principal strain distribution on bottom surface and inner cracking pattern at fatigue failure in transverse direction are shown in **Fig. 14**. The reason of choosing transverse direction is that the strain concentration can be clearly observed in this direction than that in longitudinal direction due to the effect of moving load. In this figure, the maximum principal strain can be considered as an indication of the crack opening. For all slabs, a repetition of moving load leads to an increase of tensile strain. This increasing is significant at the punching zone as shown in **Fig. 14**. The punching zone on bottom surface is assumed to be as a linear extension of loading zone with a slope equaling 45º. In other words, applying moving load leads to a significant increasing of crack opening in this zone. Therefore, the cracks are localized in the punching zone at fatigue failure. Moreover, the inner cracking pattern shows that the orientation of the distributed cracks in this zone almost equals to 45º. According to these observations, all slabs are failed as a punching shear failure. This agrees with the experimental results of the RC slabs under moving loading (Shakushiro *et al*. 2011). There are two reasons for strain concentration in the punching zone at fatigue failure. Firstly, the maximum tensile strain, $\varepsilon_{t\max}$, for the cracked elements in this zone at 1st cycle is larger than that in other elements. Secondly, the cracked elements in this zone suffered from a larger number of crack opening and closing process than other cracked elements. According to equation (1), these two factors lead to a significant concrete bridging degradation in this zone.

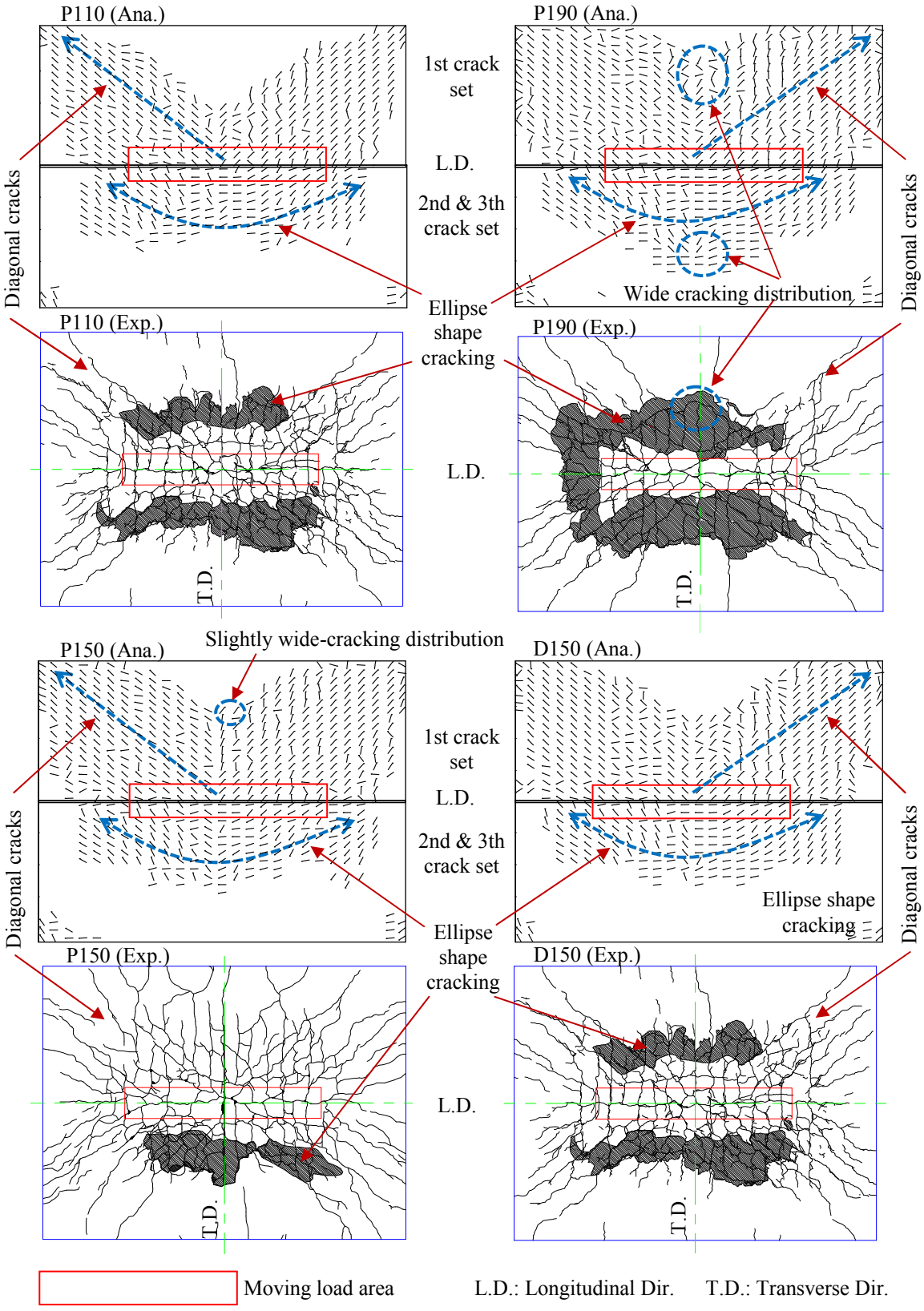

Fig.13 Cracking patterns on bottom surface for analytical and experimental RC slabs at fatigue failure.

According to **Fig. 14(c)** and **(d)**, RC slab reinforced with plain bars shows a significant increasing of maximum principal strain at fatigue failure in the punching zone than that reinforced with deformed bars. Therefore, the crack opening of the RC slab reinforced with plain bars is much larger than that reinforced with deformed bars at fatigue failure. The reason is that the modeling of bond effect between the plain bar and its surrounding concrete by reducing reinforcing bar stiffness leads to an increasing of maximum tensile strain at first cycle. By increasing number of cycles, this leads to a significant concrete bridging degradation for RC slab reinforced with plain bars resulting a higher strain at fatigue failure than that reinforced with deformed bars.

3.6 Reinforcing bars strain

This study focuses on the RC slab reinforced with plain bars under a moving load. Therefore, it is important to examine the behavior of plain bars under a moving load. To evaluate this numerical method, the strain evolutions of longitudinal and transverse lower rebar at slab center are compared with the experimental evolutions in **Fig. 15**. In all slabs, increasing number of cycles leads to an increasing of a rebar strain relatively. The reason is that the degradation of bridging stress of cracked elements with increasing number of cycles leads to an increasing of RC elements strain as shown in the equation (1). This numerical procedure simulates the cracks opening due to a repetitive of the moving load. This increasing of rebar strain is significantly observed in the RC slab un-

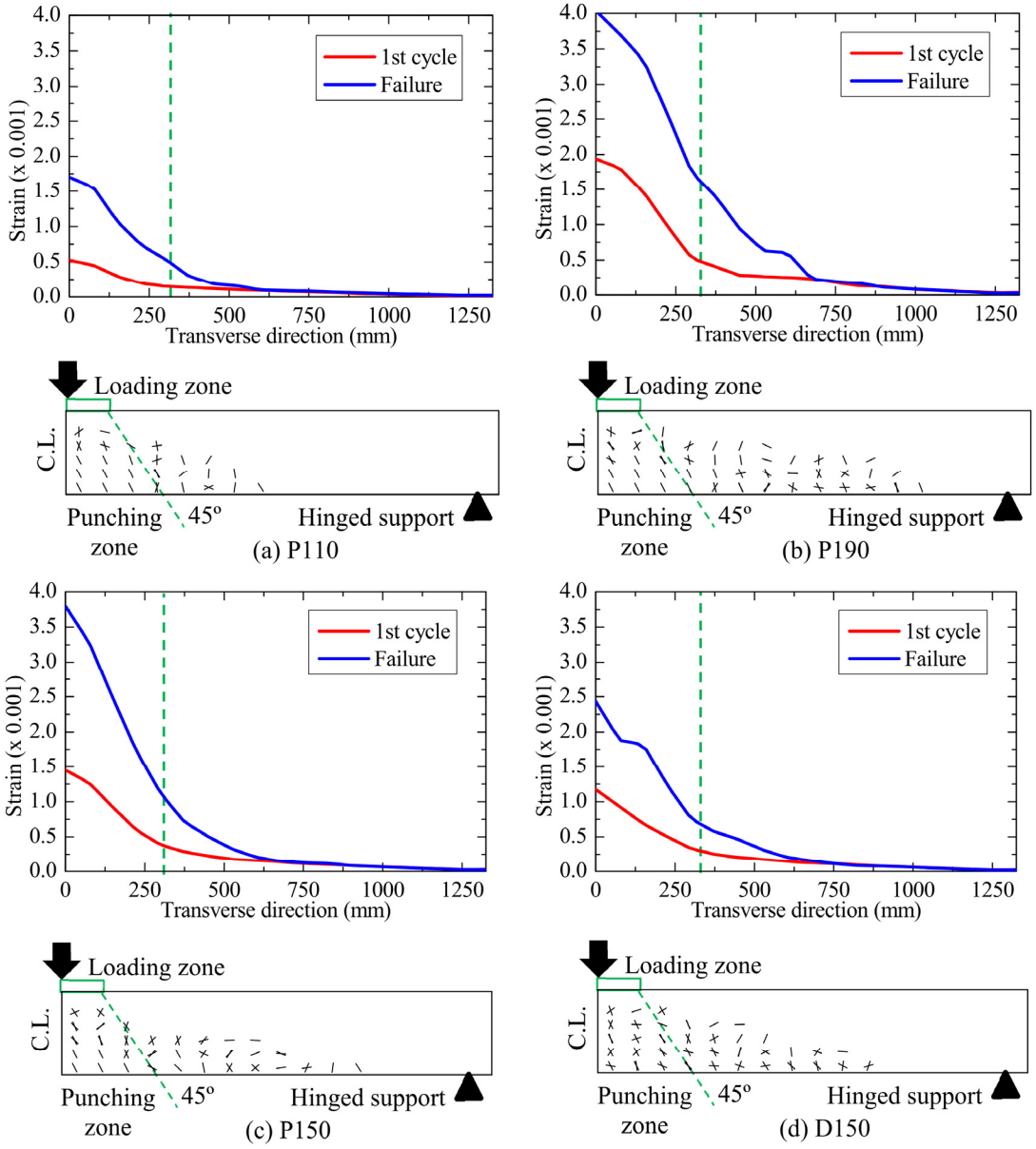

Fig.14 Maximum principal strain distribution on bottom surface and inner cracking pattern at fatigue failure in transverse direction for RC slabs under moving load.

der a higher moving load level due to its rapid propagation of the cracked elements comparing with that under a lower moving load level. For P150 and P190, the reduction in rebar stiffness in the plastic range, characterized by pinched hysteretic loops, occurred with an increasing number of cycles based on the transition parameter, R, according to the equations (6) and (7). This process leads to an additional increasing of rebar strain accordingly. Therefore, the transverse rebar strain of these slabs rises to the yield strain at the fatigue failure. According to the reinforcing bars arrangement and slab geometry in **Fig. 5(b)**, the reinforcement ratio in transverse direction (shorter length) is larger than that in longitudinal direction. Therefore, the load is distributed more along the transverse direction than in the longitudinal direction due to a higher stiffness in the transverse direction. This leads to an increasing of the rebar strain in the transverse direction than that in the longitudinal direction at the same number of cycles.

For RC slabs reinforced with plain bars, the rebar strain is calculated by the multiplying numerical strain by the explicit, ε_y, to effective, ε_y^*, yield strain ratio as shown in **Fig. 3**. This reduction of the rebar strain simulates the slipping action between the plain bar and its surrounding concrete. According to the assumptions of rebar modeling in section 2.2, the explicit, ε_y, and effective, ε_y^*, yield strain of deformed bar are with the similar value. Therefore, there is no reduction of the deformed bar strain. This explanation proves the increasing of rebar strain of RC slab reinforced with deformed bars, D150, than that reinforced with plain bars, P150, at first cycle, even though these slabs show insignificant difference in their center displacement at first cycle. By increasing the number of cycles, P150 shows a quick increasing of its rebar strain than D150 in the longitudinal and transverse directions. The reason is that the cracked elements of P150 are rapidly propagated than D150 with an increasing number of cycles as shown in **Fig. 10**.

For P110 and D150, the numerical results show an agreement with the experimental ones. For other slabs, there is a difference between the numerical and experimental results. Numerical rebar strain increases with an increasing number of cycles. However, experimental rebar strain decreases with an increasing of number of cycles. The possible reason is that the experimental measurement of a rebar strain is influenced by crack locations. Moreover, at a higher fatigue load level, the widening of the main crack causes the shrinkage in the other cracks. This leads to the decreasing of rebar strain

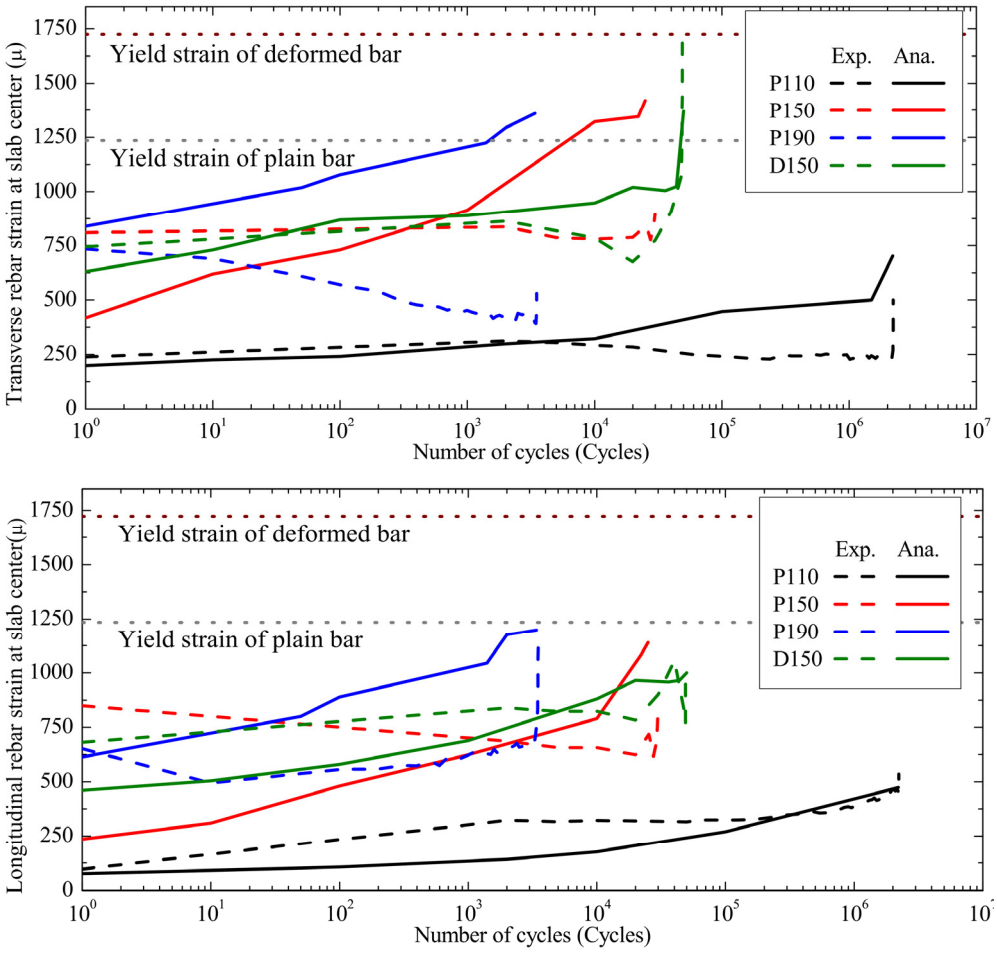

Fig.15 Lower rebar strain evolution at the slab center.

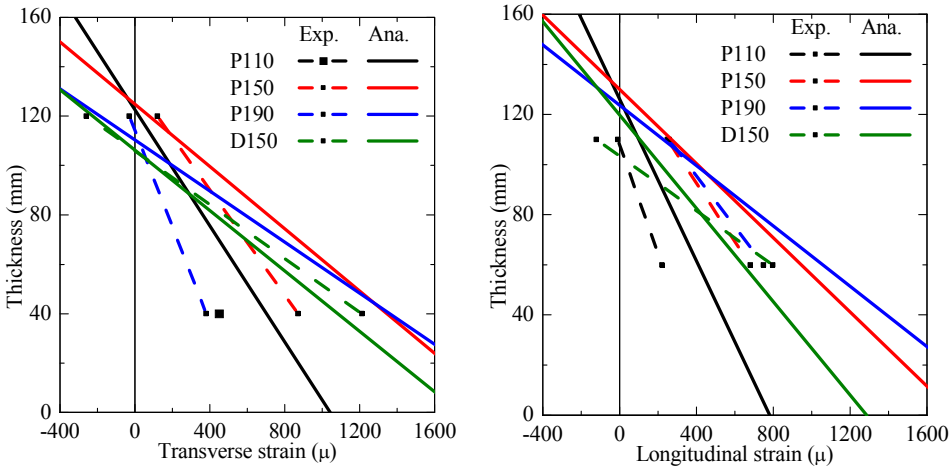

Fig.16 Strain distribution at slab center.

in the experiments.

Figure 16 shows the comparison of longitudinal and transverse sectional strain distributions with the experimental distributions for P110, P150, P190 and D150 at a selected number of cycles, N, to the number of cycles to fatigue failure, N_f, giving the ratio 0.946, 0.985, 0.97 and 0.991, respectively. These ratios are chosen to avoid the overestimated strain values in the fatigue failure. This comparison shows a difference between the numerical and experimental strain distribution for P150 and P190. Other slabs shows some agreements for numerical results. The transverse direction shows a larger strain distribution than that in the longitudinal direction. In the longitudinal and transverse directions, the strain distribution of RC slab reinforced with plain bars, P150, is a larger than that reinforced with deformed bars, D150, because this slab is degraded rapidly until the fatigue failure.

4. Conclusions

This paper showed a numerical method based on the bridging stress degradation concept to predict the fatigue behaviors of RC slabs reinforced with plain bars under a moving load.

According to this study, the applicability of the bridging stress degradation concept can be extended to predict the fatigue life of the RC slab reinforced with plain bars. The propagation of cracked elements is considered to be the primary cause of fatigue failure. By increasing the number of cycles, the bridging stress degradation of these cracked elements lead to a decrease in slab stiffness and an increase in slab deformations. Applying a moving load leads to the distribution of extensive cracks. The fatigue failure occurred when the load capacity could not exceed the moving load level. All analyzed slabs failed with the punching shear mode. This failure mode was also observed in the experiments.

The modified reinforcing bar model according to the bond-slip effect was incorporated in this numerical method. This effect shall be taken into consideration for accurate fatigue life estimations. The RC slab reinforced with plain bars shows a larger center displacement and a shorter fatigue life than that reinforced with deformed bars.

The mentioned results reveal and confirm a good agreement between the numerical analysis and the experimental results.

References

Belarbi, A. and Hsu, T. T., (1994). "Constitutive laws of concrete in tension and reinforcing bars stiffened by concrete." *ACI structural Journal*, 91(4), 465-474.

Dehestani, M. and Mousavi, S. S., (2015). "Modified steel bar model incorporating bond-slip effects for embedded element method." *Construction and Building Materials*, 81, 284-290.

Jun, Z. and Stang, H., (1998). "Fatigue performance in flexure of fiber reinforced concrete." *ACI Materials Journal*, 95(1), 58-67.

Li, V. C. and Matsumoto, T., (1998). "Fatigue crack growth analysis of fiber reinforced concrete with effect of interfacial bond degradation." *Cement and concrete composites*, 20(5), 339-351.

Maekawa, K., Okamura, H. and Pimanmas, A., (2003). "*Non-linear mechanics of reinforced concrete*." CRC Press.

Maekawa, K., Toongoenthong, K., Gebreyouhannes, E. and Kishi, T., (2006). "Direct path-integral scheme for fatigue simulation of reinforced concrete in shear." *Journal of Advanced Concrete Technology*, 4(1), 159-177.

Matsui, S. (1987). "Fatigue strength of RC-slabs of highway bridge by wheel running machine and influence of water on fatigue." *Proceedings of JCI*, 9(2), 627-632. (in Japanese)

Melo, J., Fernandes, C., Varum, H., Rodrigues, H., Costa, A. and Arêde, A., (2011). "Numerical modelling of the cyclic behaviour of RC elements built with plain reinforcing bars." *Engineering Structures*, 33(2), 273-286.

Menegotto, M. and Pinto, P. E., (1973). "Method of

analysis for cyclically loaded reinforced concrete frames including changes in geometry and non-elastic behavior of elements under combined normal forces and bending moment." IASBE Proceedings.

Perdikaris, P. C. and Beim, S., (1988). "RC bridge decks under pulsating and moving load." *Journal of Structural Engineering*, ASCE, 114(3), 591-607.

Rots, J. G. and Blaauwendraad, J. (1989). "Crack models for concrete, discrete or smeared? Fixed, multi-directional or rotating?" *HERON*, 34(1).

Shakushiro, K., (2014). "*Study on durability of highway bridge RC slabs using round bars under cyclic loading*." Thesis (Ph.D). Muroran Institute of Technology. (in Japanese)

Shakushiro, K., Mitamura, H., Watanabe, T. and Kishi, N., (2011). "Experimental study on fatigue durability of RC slabs rein-forced with round steel bars." *Journal of Structural Engineering*, JSCE, 57(A), 1297-1304, (in Japanese).

Suthiwarapirak, P. and Matsumoto, T., (2006). "Fatigue analysis of RC slabs and repaired RC slabs based on crack bridging degradation concept." *Journal of structural engineering*, ASCE, 132(6), 939-948.

Ueda, T., Zahran, M. and Kakuta, Y., (1999). "Shear fatigue behavior of steel-concrete sandwich beams." *Concrete Library International of JSCE,* 33, 83-111.

Varum, H., (2003). "Seismic assessment, strengthening and repair of existing buildings." Thesis (PhD). University of Aveiro.

Wolinski, S., Hordijk, D. A. Reinhardt, H. W. and Cornelissen, H. A., (1987). "Influence of aggregate size on fracture mechanics parameters of concrete." *International Journal of Cement Composites and Lightweight Concrete*, 9(2), 95-103.

Zhang, J., Stang, H. and Li, V. C., (1999). "Fatigue life prediction of fiber reinforced concrete under flexural load." *International Journal of Fatigue*, 21(10), 1033-1049.

Zhang, J., Stang, H. and Li, V. C., (2000). "Experimental study on crack bridging in FRC under uniaxial fatigue tension." *Journal of Materials in Civil Engineering*, ASCE, 12(1), 66-73.

Zhao, J. and Sritharan, S., (2007). "Modeling of Strain Penetration Effects in Fiber-Based Analysis of Reinforced Concrete Structures Concrete Structures." *ACI structural journal*, 104(2), 133-141.